

## Cooling-rate-dependent dielectric properties of $(\text{Pb}(\text{Mg}_{1/3}\text{Nb}_{2/3})\text{O}_3)_{0.67}(\text{PbTiO}_3)_{0.33}$ single crystals in ferroelectric phase

Feng Yan,<sup>a)</sup> Peng Bao, and Yening Wang

National Laboratory of Solid State Microstructures, Department of Physics, Nanjing University, Nanjing 210093, People's Republic of China

Helen L. W. Chan and Chung Loong Choy

Department of Applied Physics, The Hong Kong Polytechnic University, Hong Kong

(Received 8 July 2002; accepted 12 October 2002)

The dielectric properties of  $(\text{Pb}(\text{Mg}_{1/3}\text{Nb}_{2/3})\text{O}_3)_{0.67}(\text{PbTiO}_3)_{0.33}$  single crystals in the temperature range from room temperature to 250 °C have been studied. A very sharp change of dielectric permittivity due to the spontaneous relaxor–ferroelectric phase transition was observed. The most interesting result is that the dielectric permittivity in ferroelectric phase is strongly dependent on the cooling rate across the relaxor–ferroelectric phase transition. We assume that the cooling rate can influence the grain size of ferroelectric subdomains in ferroelectric phase and can therefore influence the dielectric properties. © 2002 American Institute of Physics. [DOI: 10.1063/1.1527701]

The relaxor ferroelectric materials have a very complicated phase diagram.<sup>1–3</sup> The most amazing phenomenon is the relaxor to ferroelectric (R-F) phase transition,<sup>2–10</sup> which may happen spontaneously or under high enough bias voltage. However, the tweed-like ferroelectric subdomains can be observed in the  $(\text{Pb}(\text{Mg}_{1/3}\text{Nb}_{2/3})\text{O}_3)_{0.65}(\text{PbTiO}_3)_{0.35}$  crystal<sup>11</sup> and  $(\text{Pb}_{0.93}\text{La}_{0.07})(\text{Zr}_{0.65}\text{Ti}_{0.35})\text{O}_3$  crystal<sup>11,12</sup> in ferroelectric phase, which indicates the ferroelectric phase of the relaxor is somewhat different from that of normal ferroelectrics. In this letter, the dielectric properties of  $(\text{Pb}(\text{Mg}_{1/3}\text{Nb}_{2/3})\text{O}_3)_{0.67}(\text{PbTiO}_3)_{0.33}$  (PMNT67/33) single crystal, especially during the spontaneous RF phase transition,<sup>5,11</sup> have been carefully studied.

The crystals were grown by Bridgman method<sup>13</sup> and then cut to thin pieces along (001) plane and carefully polished. Samples  $2.5 \times 2.5 \times 0.08 \text{ mm}^3$  were coated with Ag on bottom and top. The dielectric properties were measured using HP4194A impedance analyzer in a vacuum chamber in the temperature range from –100 to 300 °C, measured by a thermal couple attached to the bottom electrode.

The dielectric permittivity of PMNT67/33 along (001) was measured. The cooling rate was 3.0 °C/min and the heating rate was 1.2 °C/min. As shown in Fig. 1, a kink of dielectric permittivity appears in the temperature region  $55 \pm 10$  °C during the heating cycle, which corresponds to the phase transition from rhombohedral to tetragonal structure.<sup>5</sup> Small frequency dispersion of the dielectric permittivity below  $T_{\text{R-F}} = 147$  °C (heating cycle) indicates the sample is in ferroelectric phase in this temperature range. The dielectric permittivity shows apparent frequency dispersion above  $T_{\text{R-F}}$ . Therefore a spontaneous R-F phase transition happens at  $T_{\text{R-F}}$  and the structural change from tetragonal to cubic phase happened at the same temperature.<sup>5</sup> The two phase transitions show apparent thermal hysteresis during the cool-

ing cycle, and the transition temperature drops to  $34 \pm 10$  and 136 °C, respectively. Thus, the two phase transitions are first-order.

The most interesting result is that the cooling rate at the R-F phase transition temperature  $T_{\text{R-F}}$  has a large influence on the dielectric permittivity in the consequent ferroelectric phase, while the cooling rate in the temperature range several degrees lower or higher than  $T_{\text{R-F}}$  has no influence. As shown in Figs. 2(a) and 2(b), the sample was cooled with different rates across  $T_{\text{R-F}}$ , and the dielectric permittivity was measured in the next heating cycle with the same heating rate of 1.2 °C/min. All of the curves have little frequency dispersion below  $T_{\text{R-F}}$ , which indicates the sample is in ferroelectric phase in this temperature range for different cooling rates. The sample had the lowest dielectric permittivity in the ferroelectric phase when was quenched from 200 °C to RT, and the kink of the dielectric permittivity due to the structural phase transition happened at 55 °C disappears. The

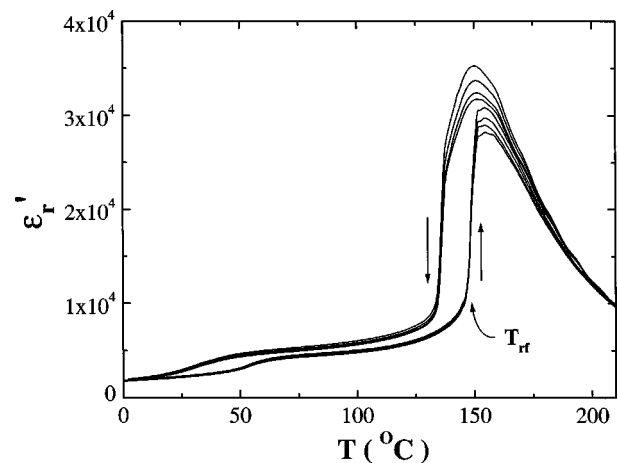


FIG. 1. The dielectric permittivity ( $\epsilon'$ ) of PMNT67/33 single crystal measured with four frequencies during cooling (rate: 3.0 °C/min) and heating (rate: 1.2 °C/min) cycles (curves from up to down for frequencies:  $10^2$ ,  $10^3$ ,  $10^4$ , and  $10^5$  Hz).

<sup>a)</sup>Current address: Department of Engineering, Cambridge University, Cambridge CB2 1PZ, UK; electronic mail: fy206@eng.cam.ac.uk

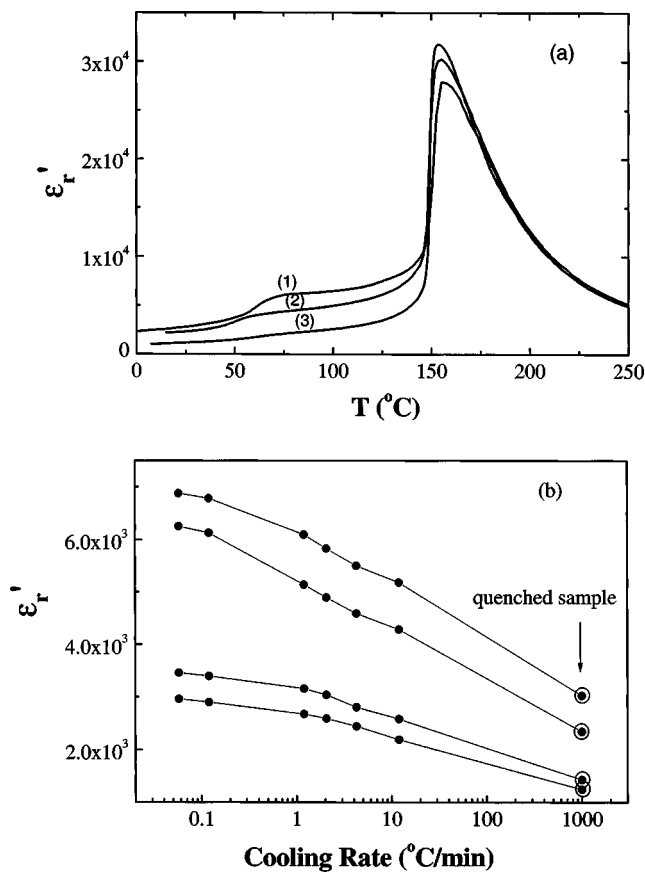


FIG. 2. (a) The dielectric permittivity ( $\epsilon'$ ) of PMNT67/33 single crystal measured in heating cycles with a same heating rate ( $1.2\text{ }^\circ\text{C}/\text{min}$ ) after a cooling cycle from  $200\text{ }^\circ\text{C}$  to RT with different cooling rate (curve 1:  $0.06\text{ }^\circ\text{C}/\text{min}$ , curve 2:  $3.0\text{ }^\circ\text{C}/\text{min}$ , and curve 3: quenched). The measurement frequency is  $10\text{ kHz}$ . (b) The cooling rate dependence of dielectric permittivity ( $\epsilon'$ ) of PMNT67/33 single crystal measured in heating process at different temperatures. (curves from up to down for temperatures:  $115$ ,  $88$ ,  $46$ , and  $32\text{ }^\circ\text{C}$ ). The measurement frequency is  $10\text{ kHz}$ . The cooling rate of the quenched sample was roughly estimated to be  $1000\text{ K}/\text{min}$ .

slower the cooling rate, the higher the dielectric permittivity can be attained below  $T_{R-F}$ . If the temperature of the sample was stabilized at  $T_{R-F}$  for  $500\text{ min}$  and then cooled at  $0.12\text{ }^\circ\text{C}/\text{min}$ , the dielectric permittivity of the sample in ferroelectric phase was higher than that of the sample was directly cooled at  $0.12\text{ }^\circ\text{C}/\text{min}$  from relaxor phase to ferroelectric phase. Thus, the time spent during the phase transition was the real factor that influenced the dielectric properties in the consequent ferroelectric phase. The dielectric permittivity in ferroelectric phase under different cooling rates was found to be very stable with time, even at a temperature just below  $T_{R-F}$ .

The effect of cooling rate cannot be explained by the spin-glass model. According to the spin-glass model,<sup>10,14–16</sup> the ferroelectric phase was induced by the long-range correlation of nanodomains. The correlated nanodomains need a certain period of time to align along a same direction, which depends on the their average relaxation time. The faster the cooling process, the shorter the ferroelectric correlation length, and thus the weaker the R-F phase transition. Thus, the sharp drop of dielectric permittivity induced by R-F phase transition should be smaller for a faster cooling rate. In other words, the dielectric permittivity in ferroelectric phase near the transition temperature  $T_{R-F}$  would be higher for a

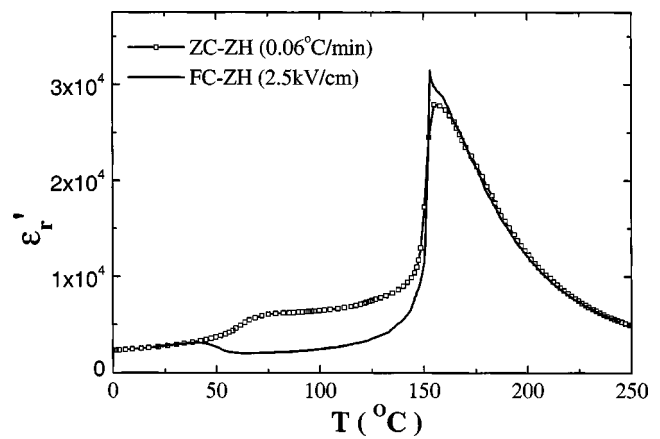


FIG. 3. The dielectric permittivity of PMNT67/33 single crystal of FC-ZH process and of ZC-ZH process with very slow cooling rate ( $0.06\text{ }^\circ\text{C}/\text{min}$ ) measured during heating process. The measurement frequency is  $10\text{ kHz}$ .

faster cooling rate, which contradicts our experimental results.

Since the ferroelectric subdomains nucleate and grow during the phase transition, we assume the average size of domains depends on the cooling rate across the phase transition, and thus the effect of cooling rate on dielectric properties may be attributed to the size effect of subdomains, similar to the grain size effect of ferroelectric ceramics.<sup>17,18</sup> The bigger the subdomains, the higher the dielectric permittivity. On the other hand, the disappearance of the phase transition from tetragonal to rhombohedral at  $55 \pm 10\text{ }^\circ\text{C}$  for the quenched sample is exactly like the grain size effect of ferroelectric ceramics with very small grain size.<sup>18</sup>

The dielectric properties of the sample during the field cooling–zero field heating (FC-ZH) process have been measured as well. The sample biased with the electric field  $2.5\text{ kV}/\text{cm}$  was cooled from  $250\text{ }^\circ\text{C}$  to RT under the cooling rate  $3.0\text{ }^\circ\text{C}/\text{min}$ , and then was heated back without bias electric field to  $250\text{ }^\circ\text{C}$  at  $1.2\text{ }^\circ\text{C}/\text{min}$ . The dielectric properties were measured during the heating process. As shown in Fig. 3, below  $45\text{ }^\circ\text{C}$ , the dielectric permittivity of the FC-ZH process almost has the same value as that of the sample of the zero field cooling–zero field heating (ZC-ZH) process cooled under very slow rate ( $0.06\text{ }^\circ\text{C}/\text{min}$ ), while it is much lower than that of ZC-ZH process from  $45$  to  $147\text{ }^\circ\text{C}$ . Above the R-F phase transition, the two curves converged again. Below  $45\text{ }^\circ\text{C}$ , the PMNT67/33 crystal is in rhombohedral phase.<sup>5</sup> The dielectric constants along  $a$ ,  $b$ , and  $c$  axes have the same value. Thus, the polarized and unpolarized samples should have the same dielectric permittivity along (001) if the size effect of subdomains was excluded. The sample of FC-ZH process has big ferroelectric subdomains below  $147\text{ }^\circ\text{C}$  for high remnant polarization can be observed. Thus, the sample of ZC-ZH process with the cooling rate  $0.06\text{ }^\circ\text{C}/\text{min}$  has the maximum dielectric permittivity below  $45\text{ }^\circ\text{C}$  and slower cooling rate cannot increase the dielectric constant any more. These results can also be considered as evidence of the size effect of ferroelectric subdomains discussed before, since a size effect always happens below a critical size.<sup>17,18</sup> Above the critical size, the dielectric permittivity is a constant value. The sample cooled at  $0.06\text{ }^\circ\text{C}/\text{min}$  must have subdomains bigger than the critical size.

From 45 to 147 °C, the PMNT67/33 crystal is in tetragonal phase. For a single domain, the dielectric constant along the *c*-axis (polarization direction)  $\epsilon_1$  is different from that along the *a*- or *b*-axis  $\epsilon_2$ . Thus, along (001), the sample polarized along (001) has the dielectric constant  $\epsilon_1$ , while the unpolarized sample has the dielectric constant  $(\epsilon_1 + 2\epsilon_2)/3$ . This is the reason the two curves in Fig. 3 separate in this temperature region.

In conclusion, the dielectric permittivity of the PMNT67/33 single crystal in ferroelectric phase was found to be strongly influenced by the cooling rate during the R-F phase transition. We assumed the size of ferroelectric subdomains in ferroelectric phase is dominated by cooling rate across the R-F phase transition, and the size effect of subdomains is the main reason for this interesting result.

<sup>1</sup>Z. Kutnjak, C. Filipic, R. Pirc, A. Levstik, R. Farhi, and M. El Marssi, Phys. Rev. B **59**, 294 (1999).

<sup>2</sup>V. Bobnar, Z. Kutnjak, R. Pirc, and A. Levstik, Phys. Rev. B **60**, 6420 (1999).

<sup>3</sup>E. V. Colla, E. Yu. Koroleva, N. M. Okuneva, and S. B. Vakhruhev, Phys. Rev. Lett. **74**, 1681 (1995).

<sup>4</sup>V. Westphal, W. Kleemann, and M. D. Glinchuk, Phys. Rev. Lett. **68**, 847 (1992).

<sup>5</sup>E. V. Colla, N. K. Yushin, and D. Viehland, J. Appl. Phys. **83**, 3298 (1998).

<sup>6</sup>G. A. Samara, Phys. Rev. Lett. **77**, 314 (1996).

<sup>7</sup>G. A. Samara, E. L. Venturini, and V. H. Schmidt, Phys. Rev. B **63**, 184104 (2001).

<sup>8</sup>X. Dai, A. DiGiovanni, and D. Viehland, J. Appl. Phys. **74**, 3399 (1993).

<sup>9</sup>F. Chu, N. Setter, and A. K. Tagantsev, J. Appl. Phys. **74**, 5129 (1993).

<sup>10</sup>R. Pirc and R. Blinc, Phys. Rev. B **60**, 13470 (1999).

<sup>11</sup>Z. Xu, M. Kim, J. Li, and D. Viehland, Philos. Mag. A **74**, 395 (1996).

<sup>12</sup>X. Dai, Z. Xu, J. Li, and D. Viehland, J. Appl. Phys. **79**, 2023 (1996).

<sup>13</sup>S. Shimanuki, S. Saito, Y. Yamashita, Jpn. J. Appl. Phys. **37A**, 3382 (1998).

<sup>14</sup>D. Viehland, J. F. Li, S. J. Jang, and L. E. Cross, Phys. Rev. B **43**, 8316 (1991).

<sup>15</sup>J. Toulouse, B. E. Vugmeister, and R. Pattnaik, Phys. Rev. Lett. **73**, 3467 (1994).

<sup>16</sup>A. Levstik, Z. Kutnjak, C. Filipic, and R. Pirc, Phys. Rev. B **57**, 11204 (1998); R. Blinc, J. Dolinsek, A. Gregorovic, B. Zalar, C. Filipic, Z. Kutnjak, A. Levstik, and R. Pirc, Phys. Rev. Lett. **83**, 424 (1999); V. Bobnar, Z. Kutnjak, R. Pirc, R. Blinc, and A. Levstik, Phys. Rev. Lett. **84**, 5892 (2000).

<sup>17</sup>G. Arlt, D. Hennings, and G. de With, J. Appl. Phys. **58**, 1619 (1985); Y. Sakashita, H. Segawa, K. Tominaga, and M. Okada, J. Appl. Phys. **73**, 7857 (1993).

<sup>18</sup>W. Zhong, P. Zhang, Y. Wang, and T. Ren, Ferroelectrics **160**, 55 (1995).

Applied Physics Letters is copyrighted by the American Institute of Physics (AIP). Redistribution of journal material is subject to the AIP online journal license and/or AIP copyright. For more information, see <http://ojps.aip.org/aplo/aplcr.jsp>  
Copyright of Applied Physics Letters is the property of American Institute of Physics and its content may not be copied or emailed to multiple sites or posted to a listserv without the copyright holder's express written permission. However, users may print, download, or email articles for individual use.